



*Supplement of*

**Insights into the long-term (2005–2021) spatiotemporal evolution of summer ozone production sensitivity in the Northern Hemisphere derived with the Ozone Monitoring Instrument (OMI)**

**Matthew S. Johnson et al.**

*Correspondence to:* Matthew S. Johnson ([matthew.s.johnson@nasa.gov](mailto:matthew.s.johnson@nasa.gov))

The copyright of individual parts of the supplement might differ from the article licence.

Supplemental Figures

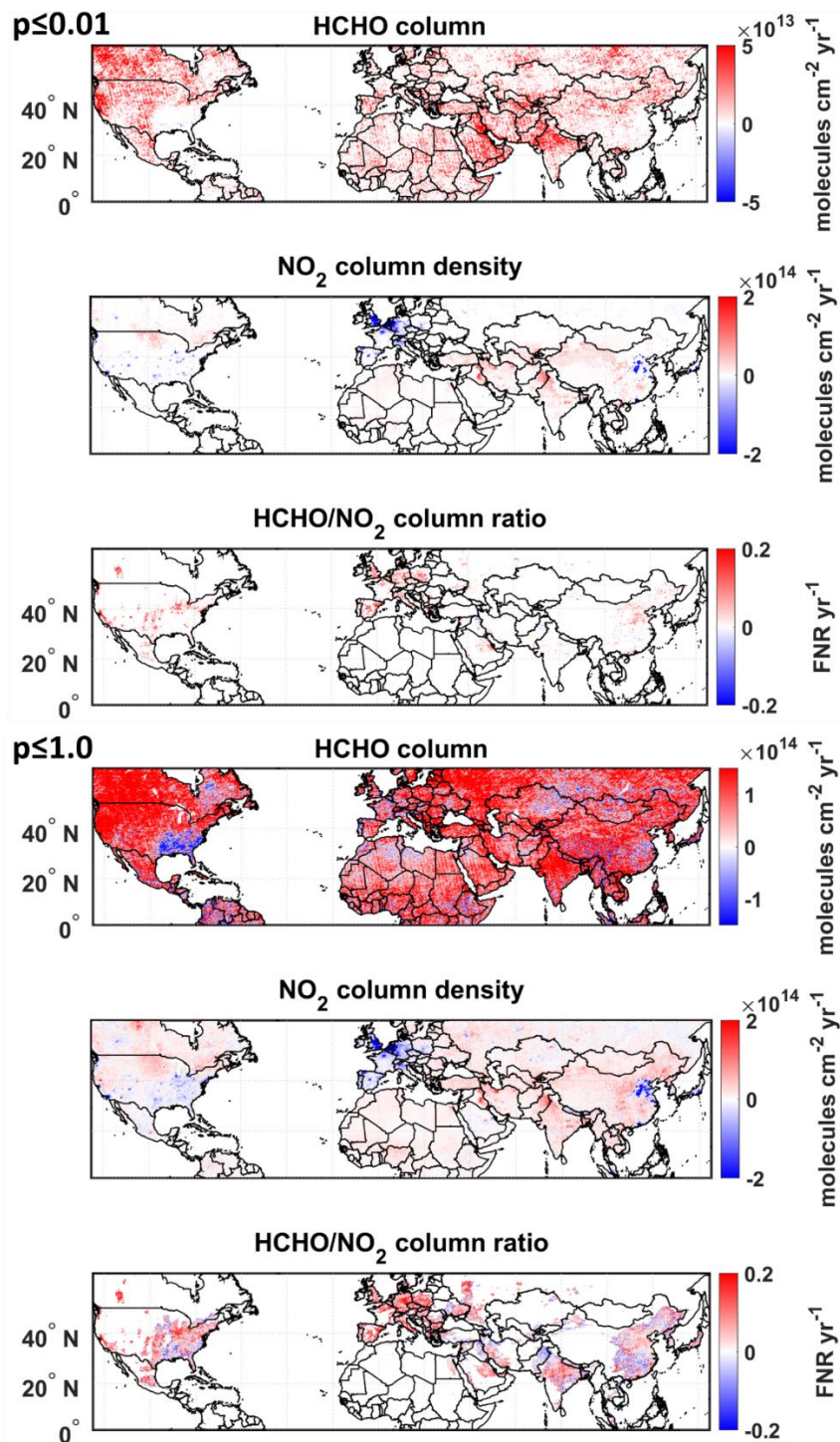


Figure S1. OMI-derived trends in summer mean (June-August) HCHO (top row) and  $\text{NO}_2$  (middle row) VCDs (left column; units in molecule  $\text{cm}^{-2} \text{yr}^{-1}$ ), and corresponding FNR values (bottom row; unitless  $\text{yr}^{-1}$ ) at  $0.1^\circ \times 0.1^\circ$  latitude  $\times$  longitude grid cells between 2005 and 2021. Values in the bottom row are displayed only for polluted regions (OMI  $\text{NO}_2$  VCD  $> 1.2 \times 10^{15}$  molecule  $\text{cm}^{-2}$ ). The white color indicates data gaps or oceanic grid cells. All trend values that are displayed are at a 99% confidence level (top panels) and for all grid cells (bottom panels).

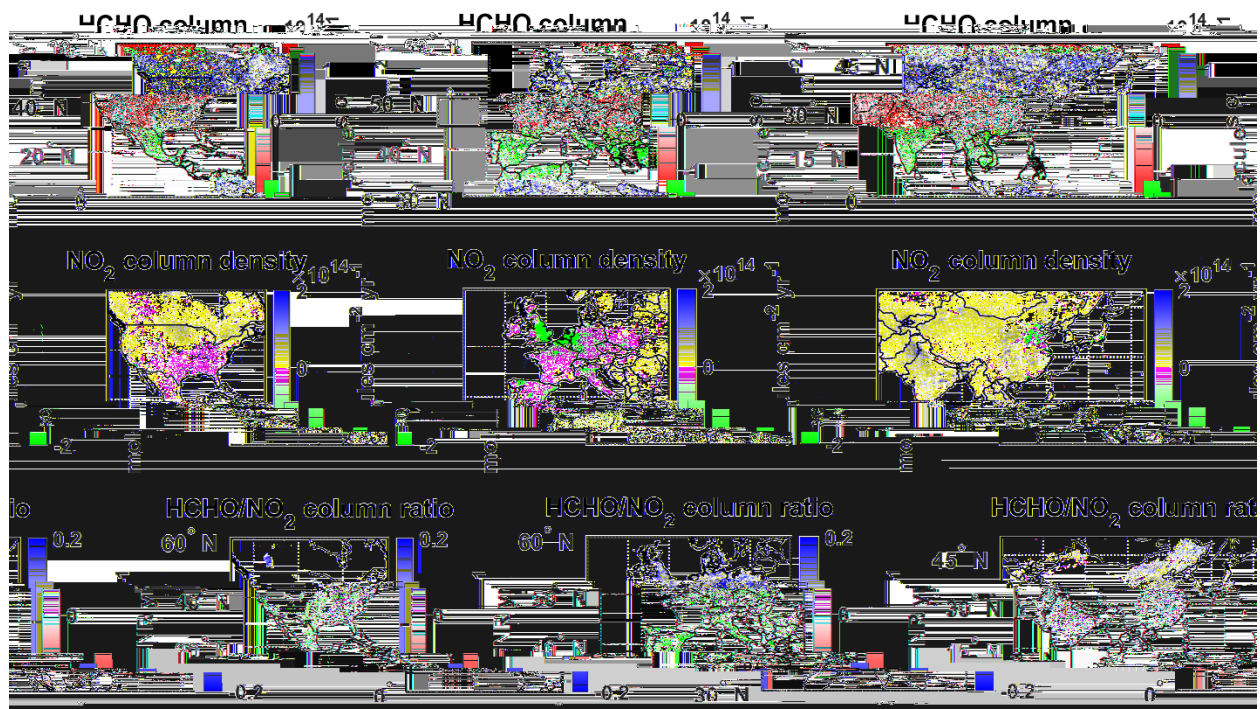


Figure S2. OMI-derived trends in summer mean (June-August) time series of HCHO (top row) and NO<sub>2</sub> (middle row) VCDs (units in molecule cm<sup>-2</sup> yr<sup>-1</sup>), and corresponding FNR values (bottom row; unitless yr<sup>-1</sup>) at 0.1° × 0.1° latitude × longitude grid cells between 2005 and 2021 for North America (left column), Europe (middle column), and Asia (right column). Values in the bottom row are displayed only for polluted regions (OMI NO<sub>2</sub> VCD > 1.2 × 10<sup>15</sup> molecule cm<sup>-2</sup>). The white color indicates data gaps or oceanic grid cells. All trend values that are displayed are at an 85% confidence level ( $p \leq 0.15$ ) for better visualization of spatial trend variability.

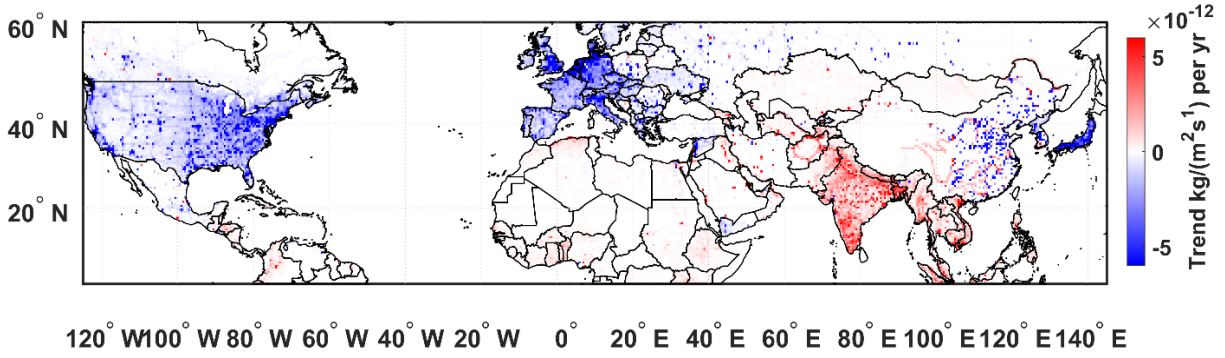
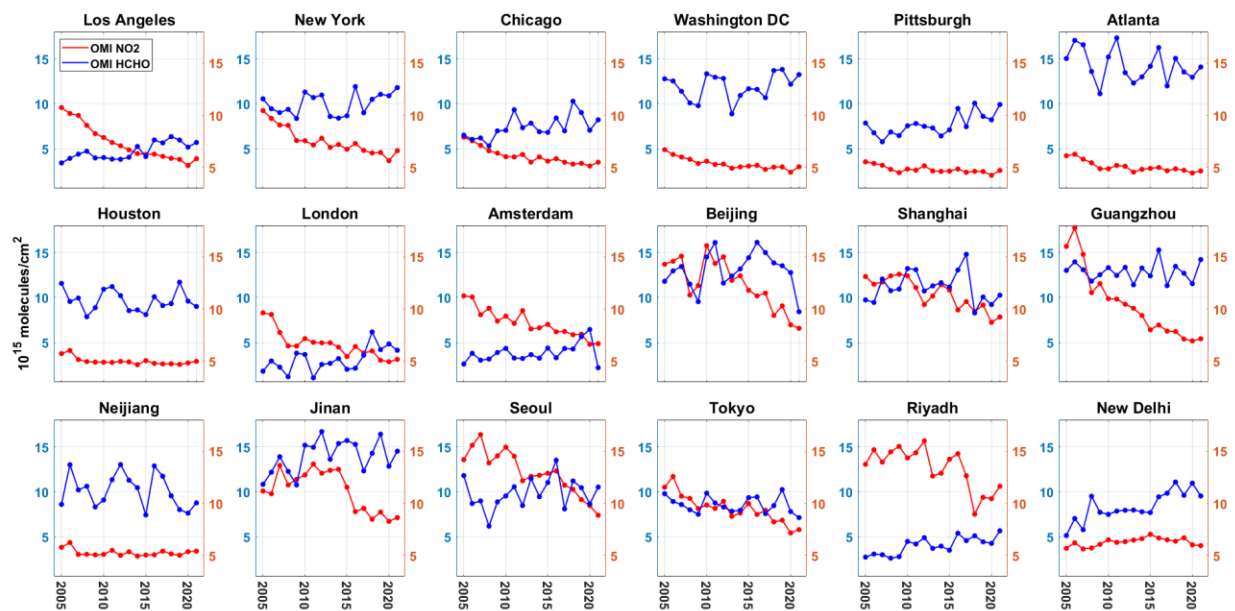


Figure S3. Trend in CEDS anthropogenic NO<sub>x</sub> emission ( $\text{kg m}^{-2} \text{s}^{-2} \text{ yr}^{-1}$ ) between 2005-2019. Values are displayed for grids with statistically significant trends at a 95% ( $p \leq 0.05$ ) confidence level.



**Figure S4. Time series of OMI-derived summer mean (June-August) VCD NO<sub>2</sub> and HCHO abundances (10<sup>15</sup> molecules cm<sup>-2</sup>) for 18 selected cities across the North Hemisphere from 2005 to 2021.**

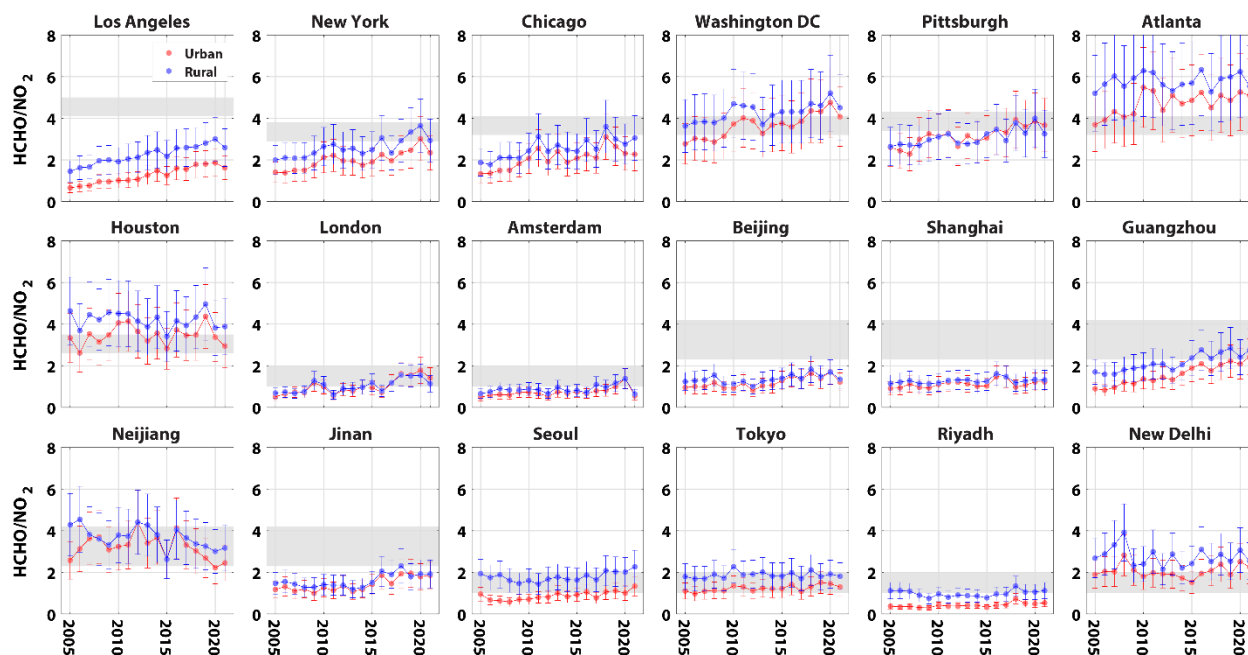


Figure S5. Time series of OMI-derived summer mean (June-August) FNR VCD values for 18 selected cities across the North Hemisphere from 2005 to 2021. The OMI HCHO version 3 collection 3 data has been detrended to remove the positive drift in this product. The different colors illustrate mean FNR values for urban (red) and rural areas around each city (blue). Grey shaded areas represent the transition zone of ozone production sensitivity regime threshold values as suggested by Jin et al. (2020) (cities in United States: Los Angeles, New York, Chicago, Washington DC, Pittsburgh, Atlanta and Houston), Wang et al. (2021) (cities in China: Beijing, Shanghai, Guangzhou, Neijiang and Jinan), and Duncan et al. (2010) (other cities). For interpretation, FNR values that are less than the transition zone have  $O_3$  production which is VOC-limited and FNR values larger than the transition zone have  $O_3$  production which is  $NO_x$ -limited.

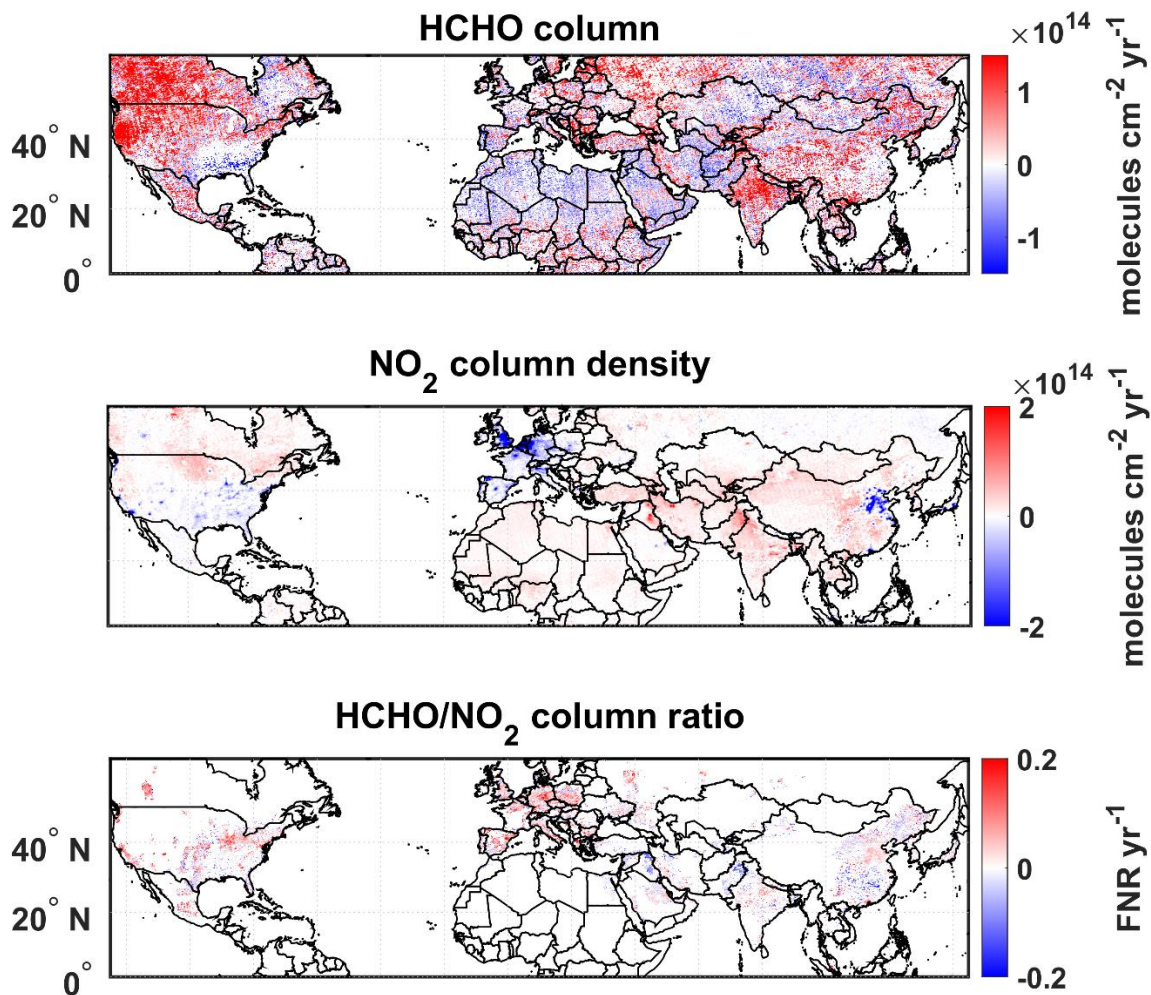
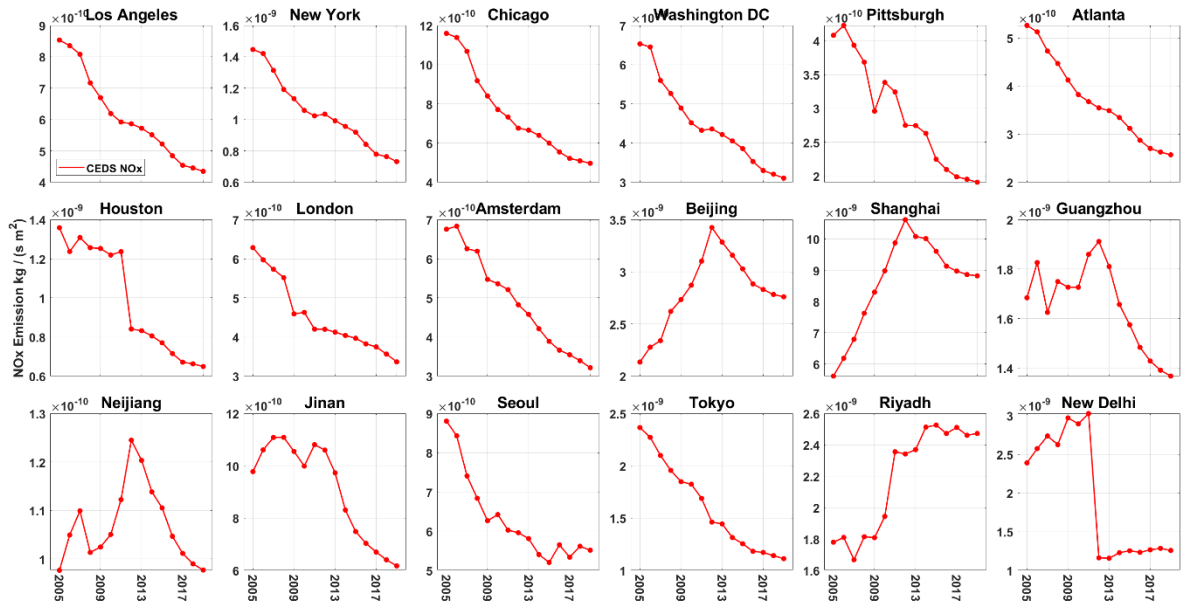


Figure S6. OMI-derived trends in summer mean (June-August) time series of HCHO (top row) and NO<sub>2</sub> (middle row) VCDs (units in molecule  $\text{cm}^{-2} \text{yr}^{-1}$ ), and corresponding FNR values (bottom row; unitless  $\text{yr}^{-1}$ ) at  $0.1^\circ \times 0.1^\circ$  latitude  $\times$  longitude grid cells between 2005 and 2021. The OMI HCHO version 3 collection 3 data is detrended in these images. Values in the bottom row are displayed only for polluted regions (OMI NO<sub>2</sub> VCD  $> 1.2 \times 10^{15}$  molecule  $\text{cm}^{-2}$ ). The white color indicates data gaps or oceanic grid cells. All trend values that are displayed are at an 85% confidence level ( $p \leq 0.15$ ) for better visualization of spatial trend variability.



**Figure S7. Time series of CEDA summer mean (June-August) anthropogenic NO<sub>x</sub> emissions (kg NO<sub>x</sub> s<sup>-1</sup> m<sup>-2</sup>) for 18 selected cities across the North Hemisphere from 2005 to 2019.**



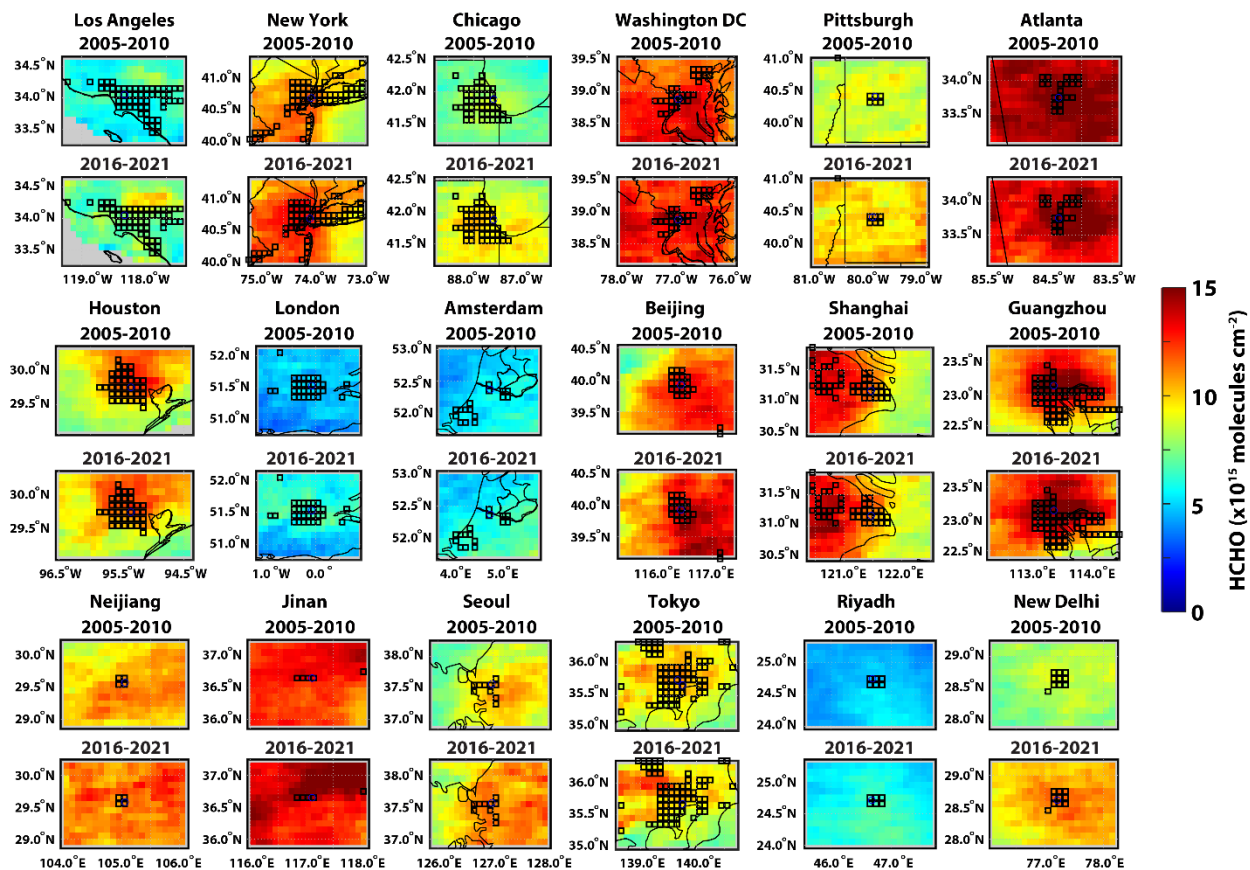


Figure S8. OMI-derived summer mean (June-August) HCHO VCD values for 18 selected cities across the Northern Hemisphere during 2005-2010 and 2016-2021. Outlined black squares represent CGLZ urban defined grid points.

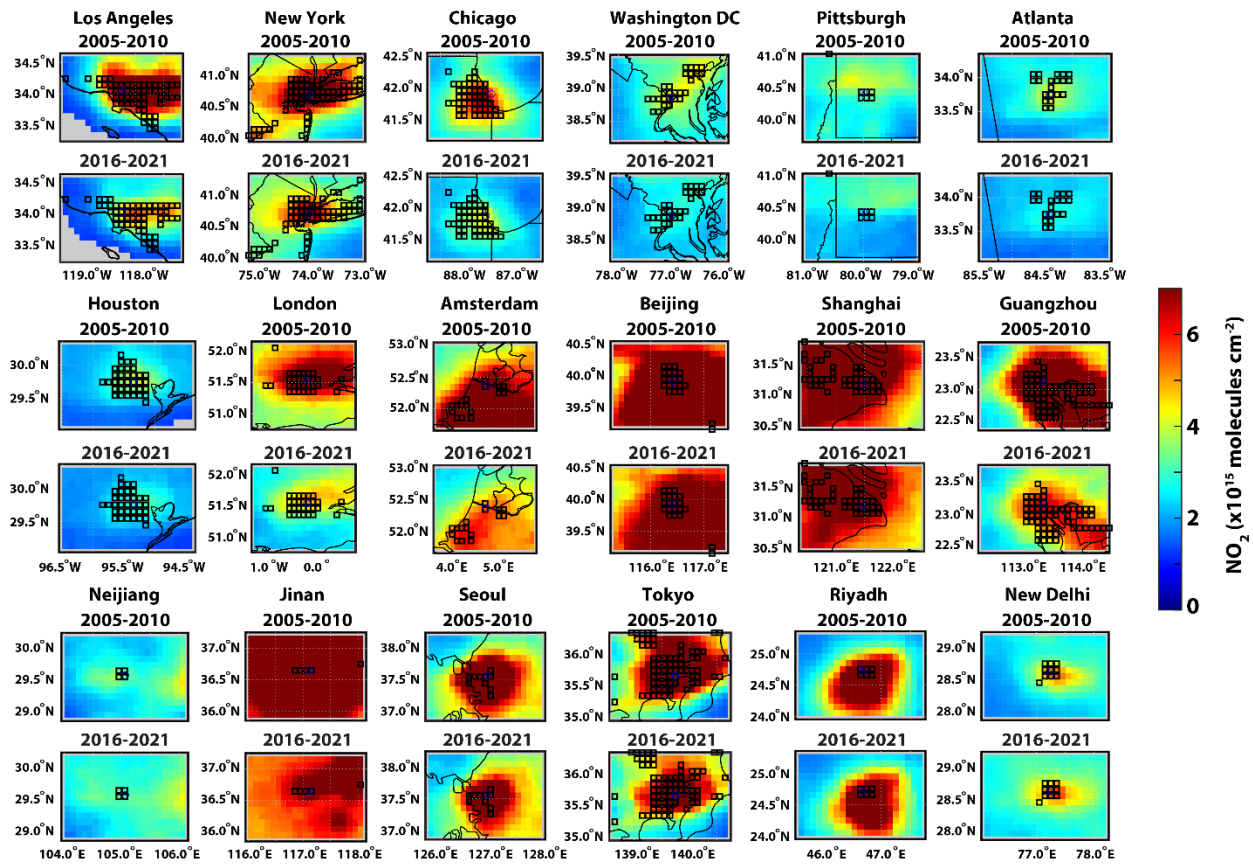


Figure S9. OMI-derived summer mean (June-August) NO<sub>2</sub> VCD values for 18 selected cities across the Northern Hemisphere during 2005-2010 and 2016-2021. Outlined black squares represent CGLZ urban defined grid points. Grey color indicates data gaps or oceanic grid cells.

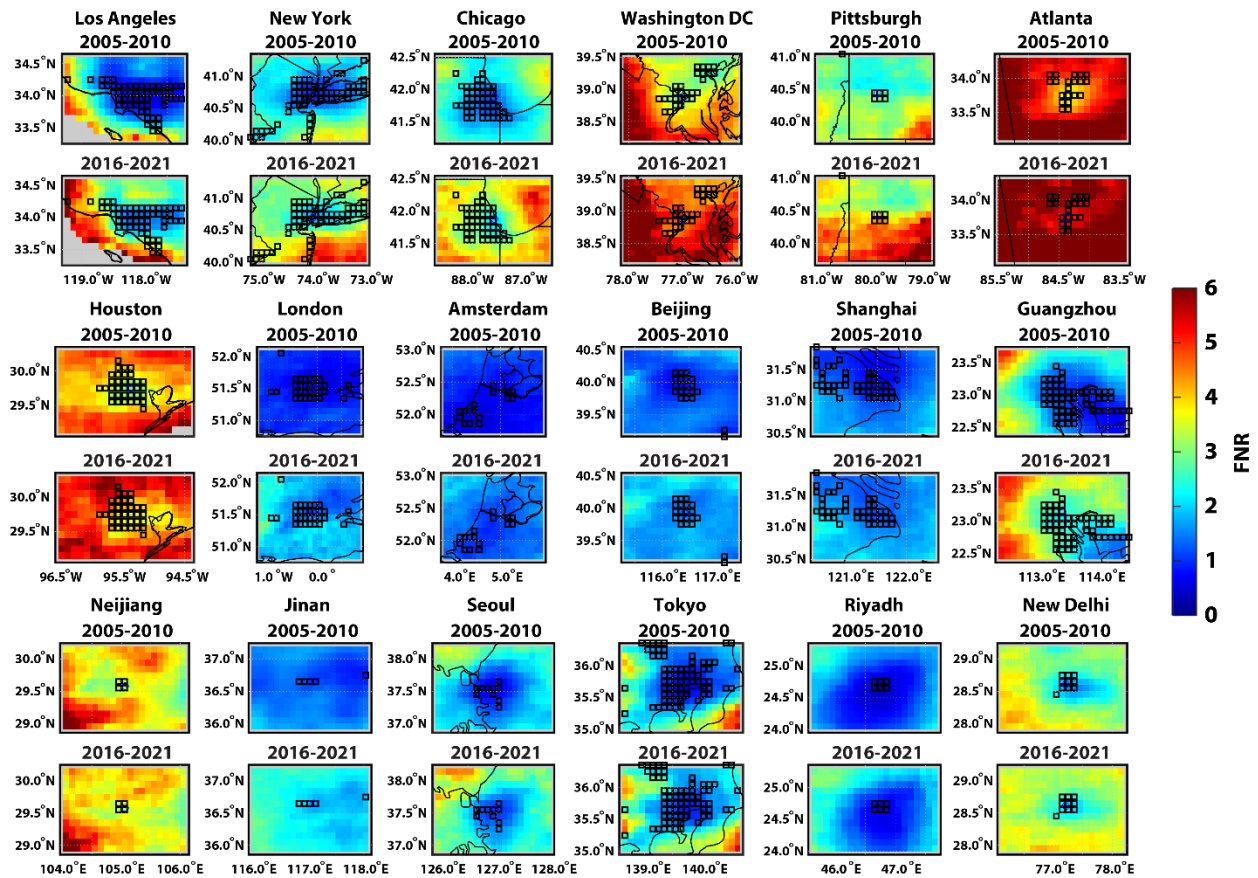


Figure S10. OMI-derived summer mean (June-August) FNR VCD values for 18 selected cities across the Northern Hemisphere during 2005-2010 and 2016-2021. The black squares represent the CGLC-MODIS-LCZ urban defined grids for each city. Grey color indicates data gaps or oceanic grid cells.